

# Time–temperature relations for the remagnetization of pyrrhotite ( $\text{Fe}_7\text{S}_8$ ) and their use in estimating paleotemperatures

D.J. Dunlop<sup>a,\*</sup>, Ö. Özdemir<sup>a</sup>, D.A. Clark<sup>b</sup>, P.W. Schmidt<sup>b</sup>

<sup>a</sup> *Geophysics, Physics Department, University of Toronto, Toronto, Ont., M5S 1A7, Canada*

<sup>b</sup> *CSIRO Division of Exploration and Mining, North Ryde, Sydney 2113, Australia*

Received 28 September 1999; received in revised form 1 December 1999; accepted 1 December 1999

## Abstract

Paleotemperature controls the maturation of coal and hydrocarbons in sedimentary basins and is also important in determining paleogeothermal gradient and hence tectonic style in exhumed metamorphic terrains. One method of estimating paleotemperature analyses the partial remagnetization of a rock due to heating in thick volcanic or sedimentary sequences, over subcrustal heat sources such as plumes, or at convergent plate margins. The overprinted natural remanent magnetization (NRM) of a rock records both the age and the paleotemperature of remagnetization, but a temperature correction from laboratory to geological time scales is required, using theoretical time–temperature relations. Time–temperature relations are well known for magnetite ( $\text{Fe}_3\text{O}_4$ ) but are reported here for the first time for pyrrhotite ( $\text{Fe}_7\text{S}_8$ ), another common NRM carrier. Data for each mineral separately yield independent estimates of paleotemperature if geologically reasonable estimates of heating time can be made. Paleotemperature can be estimated without geological input if data for both minerals are combined. Together with the age of remagnetization, determined from the paleomagnetic pole of the NRM overprint, these paleotemperature estimates can be used to infer the history of heating and uplift following burial. As a test case, we examine thermally acquired NRM overprints carried by pyrrhotite ( $\text{Fe}_7\text{S}_8$ ) and magnetite ( $\text{Fe}_3\text{O}_4$ ) in the Milton Monzonite of southeastern Australia. These overprints record a heating event about 100 Ma ago, probably thermal doming prior to rifting of the Tasman Sea, that upgraded coal rank in the Sydney Basin. Extrapolating from laboratory to geological times, using the new time–temperature contours for pyrrhotite, we estimate that the presently exposed Sydney Basin in the vicinity of the Milton Monzonite was remagnetized by heating to  $165 \pm 30^\circ\text{C}$  for  $\approx 100$  ka. Assuming a paleogeothermal gradient of  $70^\circ\text{C}/\text{km}$  appropriate for young or incipient rifts, the depth of burial at the time of remagnetization is estimated to have been  $2.3 \pm 0.4$  km. This figure is in excellent agreement with independent estimates based on reflectance data for the coal accessory mineral vitrinite. © 2000 Elsevier Science B.V. All rights reserved.

**Keywords:** paleotemperature; remagnetization; pyrrhotite; magnetite; P-T-t paths

## 1. Introduction

Knowledge of paleotemperatures in sedimentary basins is important because thermal history

\* Corresponding author. Tel.: +1-905-828-3968;  
Fax: +1-905-828-3717; E-mail: dunlop@physics.utoronto.ca

controls the maturation of coal and hydrocarbons [1]. Paleotemperatures are also needed to infer paleogeothermal gradient and tectonic history of uplifted terrains, such as those originally formed at convergent plate margins (low thermal gradient) or in rifted margin environments (high thermal gradient). Many geothermometers are in common use, among them coal rank and reflectance of vitrinite, a coal accessory mineral [1], clay mineral diagenesis [2], conodont and acritarch color alteration [3], metamorphic mineral assemblages [4], and reset  $^{40}\text{Ar}/^{39}\text{Ar}$  and fission track ages [5,6]. Most of these apply to specific rock types over limited temperature ranges.

Another relatively unrestricted geothermometer uses remagnetization temperatures of natural remanent magnetization or NRM [1,7–15]. Thermal overprinting of NRM can occur in any rock type over broad temperature ranges: 20–580°C for magnetite ( $\text{Fe}_3\text{O}_4$ ) or 20–320°C for monoclinic pyrrhotite ( $\text{Fe}_7\text{S}_8$ ). Most continental rocks contain one or other of these minerals. A further advantage of the thermal remagnetization method is that the time of heating can also be found, by comparing the paleomagnetic pole of the NRM overprint to a known apparent polar wander path.

## 2. The thermal remagnetization geothermometer

The remagnetization geothermometer [7] is based on the Néel [16] theory of magnetic single-domain grains. At absolute temperature  $T$ , the relaxation time  $\tau$  for thermally activated magnetization changes in weak fields is:

$$1/\tau = C \exp[-\mu_0 V H_{K0} M_{s0} \beta^n(T) / 2kT] \quad (1)$$

where  $C = 10^9\text{--}10^{10} \text{ s}^{-1}$ ,  $\mu_0 = 4\pi \times 10^{-7} \text{ H/m}$ ,  $V$  and  $H_K$  are grain volume and coercive force,  $\beta(T)$  is the normalized  $T$  dependence of spontaneous magnetization  $M_s$ ,  $n$  depends on the mechanism of anisotropy, and  $k$  is Boltzmann's constant.  $H_{K0}$  and  $M_{s0}$  are the values of  $H_K$  and  $M_s$  at room temperature  $T_0$ . Because  $\tau$  depends exponentially on  $T$  and  $\beta(T)$ , grains with a particular  $V$  and  $H_{K0}$  will acquire a permanent NRM when

they are cooled a few °C through their blocking temperature  $T_B$ , at which  $\tau \approx t$ , a typical experimental time. The NRM of the same grains will be thermally demagnetized when reheated through the unblocking temperature  $T_{UB}$ , at which  $\tau$  is again  $\approx t$ .

In nature, a thermal NRM overprint is acquired at a remagnetization temperature  $T_B = T_r$  over a time interval  $t_r$  of geological length, whereas in laboratory heatings for short time intervals  $t_L$ , thermal demagnetization occurs at a higher temperature  $T_{UB} = T_L$ . The last grains to be magnetized in nature and demagnetized in the laboratory are those with the largest value of  $VH_{K0}$ . For these grains, Eq. 1 gives the remagnetization relation [7]:

$$T_r \beta_r^{-n} \ln(Ct_r) = T_L \beta_L^{-n} \ln(Ct_L) = \mu_0 V H_{K0} M_{s0} / 2k \quad (2)$$

in which subscripts r, L and 0 refer to values at  $T_r$ ,  $T_L$  and  $T_0$ , respectively. (For an equivalent relation in continuous heating/cooling, see [8].)

Fig. 1 is a contour plot of  $T\beta^{-n}(T)\ln(Ct)$  for various values of the constant  $\mu_0 V H_{K0} M_{s0} / 2k$ . Possible combinations ( $T_r$ ,  $t_r$ ) of geological remagnetization temperature and time can be found by following the contour passing through the point ( $T_L$ ,  $t_L$ ) determined from laboratory thermal demagnetization of a thermal overprint. A unique solution ( $T_r$ ,  $t_r$ ) is given by intersecting contours for two minerals with different  $M_s(T)$ .

Contours for single-domain magnetite and hematite ( $\alpha\text{Fe}_2\text{O}_3$ ) are known [7], but the  $T$ - $t$  contours for pyrrhotite are reported here for the first time (see also [17,18]). For  $\text{Fe}_7\text{S}_8$ , we used a molecular field approximation  $\beta(T) = 1.48(1 - T/T_C)^{0.52}$  with a measured Curie temperature  $T_C = 593 \text{ K}$  (320°C) and  $n = 2.6$  [19,20]. This  $\beta$  function and  $n$  value give good fits to  $M_s$  and coercive force data for single-domain and small pseudo-single-domain  $\text{Fe}_7\text{S}_8$  over most of the range ( $T_0$ ,  $T_C$ ). We also recalculated contours for magnetite, using  $\beta(T) = 1.193(1 - T/T_C)^{0.42}$  with  $T_C = 853 \text{ K}$  (580°C), which gives a reasonable fit to  $M_s(T)$  measurements [21], and  $n = 2$ , for single-domain grains with shape anisotropy.

The  $T$ - $t$  contours for both minerals are steep

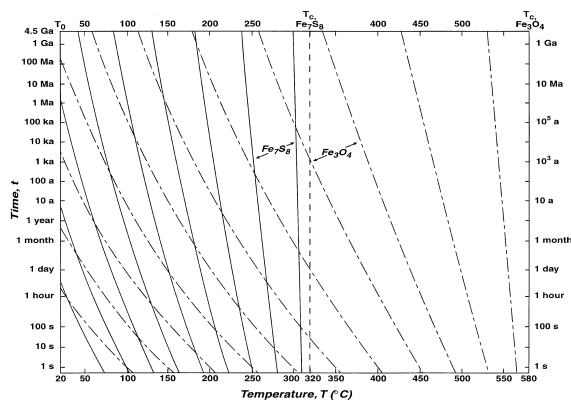


Fig. 1. Time vs. temperature contours calculated for pyrrhotite ( $\text{Fe}_7\text{S}_8$ ) and magnetite ( $\text{Fe}_3\text{O}_4$ ). Blocking or unblocking temperatures of magnetization for a particular ensemble of single-domain grains can be determined as a function of time by following one of the contours. Below the pyrrhotite Curie point,  $T_C = 320^\circ\text{C}$ , magnetite and pyrrhotite contours defined by laboratory thermal demagnetization data intersect to give a unique determination of the remagnetization time and temperature in nature.

near the Curie temperature  $T_C$ , where  $M_s$  changes rapidly, and more gently sloping at lower temperatures. Because the Curie points of pyrrhotite and magnetite differ by more than  $250^\circ\text{C}$ , sloping magnetite contours and steeper pyrrhotite contours intersect at reasonably large angles in the range  $20\text{--}300^\circ\text{C}$  (Fig. 1). We can therefore determine remagnetization temperatures up to  $300^\circ\text{C}$  fairly accurately if we have thermal demagnetization data for thermal overprints from both these minerals, or data from pyrrhotite alone plus an estimate of geological heating time.

### 3. An example of the pyrrhotite remagnetization method: the Milton Monzonite

To illustrate both approaches, we will use paleomagnetic data from the Milton Monzonite [22,23], an early Triassic intrusion into flat-lying sediments of the Sydney Basin (Fig. 2). This example provides an ideal test of our calculations of paleotemperature for several reasons. First, the paleomagnetic results indicate thermal overprinting of both pyrrhotite and magnetite, as described below. Second, the Sydney Basin has a simple

history: subsidence from Permian to early Jurassic, with deposition of several km of marine sediments and coal measures, followed by quiescence until thermal doming and initial rifting of the Tasman Sea caused rapid uplift and erosion 100–70 Ma ago. Finally, vitrinite reflectance measurements on coal deposits [1] provide independent estimates of paleotemperature and burial depth to which we can compare our results.

Thermal demagnetization was carried out using three non-inductive resistance furnaces in a field-free space, each furnace containing  $\approx 20$  cylindrical cores 2.5 cm in diameter. While one furnace was heating, another was cooling, and the specimens from the third were being measured on a SQUID magnetometer. Heatings were programmed using a controller that gave negligible

### Vitrinite reflectance contours

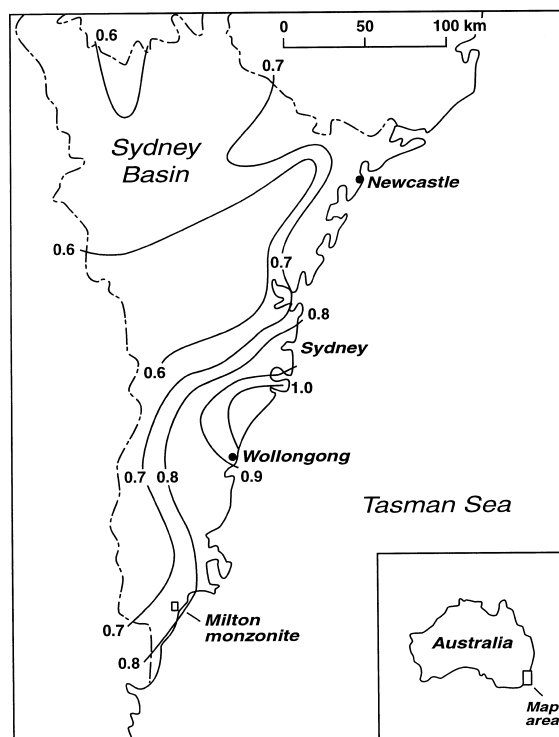


Fig. 2. Map of the Sydney Basin, Australia, showing contours of vitrinite reflectance of surface rocks in % (after [1]) and the location of the Milton Monzonite. Vitrinite reflectance and coal rank increase towards the Tasman Sea coast, indicating deeper levels of burial or a higher paleogeothermal gradient prior to rifting.

temperature overshoot. The time required for specimens to reach a uniform temperature throughout their volumes was determined to be 5–10 min by comparing surface and interior temperatures read by two thermocouples, one cemented to the surface of a dummy sample and the other embedded in its center. This equilibration time was used for the hold time at temperature  $T$  and is used later as the value of  $t_L$ . The value of  $T$  used in calculations is the average of the surface and interior thermocouple readings. Within each furnace, temperatures were quite uniform. Nevertheless, specimens were returned to the same positions for all heatings.

Magnetite is the usual NRM carrier in the Mil-

ton Monzonite (Fig. 3, left). However, at two sites, pyrrhotite carries both the primary NRM and a thermal overprint (Fig. 3, right; see also [22] Fig. 5). The primary NRM of sample 7g2 (labelled HT for higher temperature in Fig. 3) has  $T_{UB}$  values up to  $\approx 313^\circ\text{C}$ , just below  $320^\circ\text{C}$ , the Curie point of pyrrhotite. The pyrrhotite overprint (labelled LT for lower temperature) has lower  $T_{UB}$ 's that do not overlap those of the primary NRM, with the result that the HT and LT vector projections have a sharp intersection with no rounding indicative of overlap of  $T_{UB}$ 's. (There is also an overprint evident in Fig. 3 carried by magnetite, with a direction similar to LT but higher  $T_{UB}$  values than either LT or HT. It is

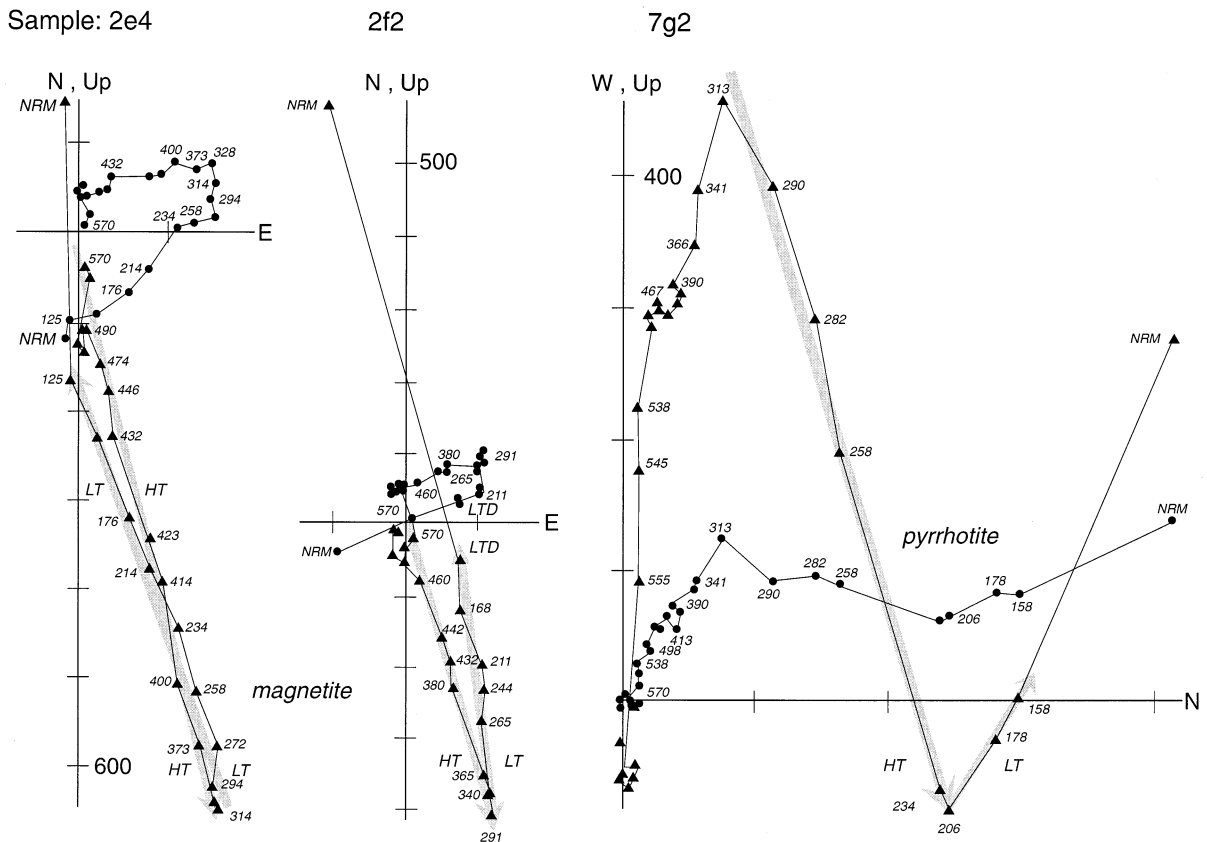


Fig. 3. Examples of vector plots of thermal demagnetization data (temperatures in  $^\circ\text{C}$ ) for samples of the Milton Monzonite. Vertical and horizontal plane projections of the NRM vector are denoted by triangles and circles, respectively. Samples 2e4 and 2f2 have both the primary HT and thermally overprinted LT vectors carried by magnetite. Prior LTD of 2f2 reduces its LT–HT junction temperature to  $291^\circ\text{C}$ , much below that of companion specimens. In sample 7g2, LT and HT are carried by pyrrhotite. A magnetite chemical overprint with approximately the same direction as LT is evident above  $313^\circ\text{C}$  but is irrelevant to the discussion in this paper.

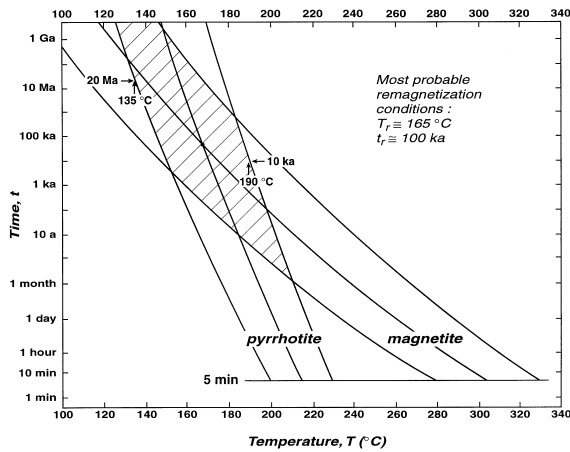


Fig. 4. Determining the remagnetization conditions ( $T_r$ ,  $t_r$ ) under which the Milton LT overprint was acquired in nature by extrapolating from laboratory ( $T_L$ ,  $t_L$ ) data for pyrrhotite- and magnetite-bearing samples, using the ( $T$ ,  $t$ ) contours of Fig. 1. When pyrrhotite carries the overprint, the observed range of  $T_L$  values in thermal demagnetization ( $t_L = 5$  min) is 200–230°C. On geological timescales, this translates into upper and lower bounds on  $T_r$  of 135–190°C. The most probable remagnetization conditions are given by the intersection of the average pyrrhotite and magnetite contours:  $T_r \approx 165^\circ\text{C}$  and  $t_r \approx 100$  ka. The shaded region between the maximum and minimum pyrrhotite and magnetite contours contains all theoretically permitted ( $T_r$ ,  $t_r$ ) combinations, but lengths of geomagnetic polarity epochs and realistic uplift rates impose upper and lower limits on  $t_r$ . Our paleomagnetic estimates of  $T_r$  are in good agreement with independent estimates from vitrinite reflectance [1].

not relevant to our discussion because it is of chemical rather than thermal origin [22].) The non-overlapping  $T_{UB}$  ranges of the overprinting (LT) and overprinted (HT) components are diagnostic of thermal overprinting in single-domain grains [21,24,25].

The HT vector direction defines a paleomagnetic pole older than 200 Ma, whereas the overprint paleopole is about 100 Ma in age [22]. The overprint is ubiquitous throughout the Sydney Basin and was probably acquired during uplift associated with opening of the Tasman Sea. Judging by the junction temperature between the LT and HT vectors (Fig. 3, right), grains with laboratory  $T_{UB}$  values up to 206°C have been overprinted. Thus  $T_L$  for this sample is 206°C. By way of comparison, the junction temperature for sample 7d2 ([22] fig. 5) was 222°C.

Values of maximum unblocking temperature  $T_L$  for all the pyrrhotite-bearing samples are in the range 200–230°C ([23] fig. 2, 17 determinations). For the equilibration time at  $T_L$  during thermal demagnetization, we used the furnace hold time:  $t_L \approx 5$  min (see above). The pyrrhotite contours through the extremes (5 min, 200°C) and (5 min, 230°C) outline the region of permitted ( $t$ ,  $T$ ) combinations in remagnetization (Fig. 4).

Geomagnetic and geological constraints narrow the range of possible  $t_r$  values, and therefore also  $T_r$  values. To be measurable as a single NRM vector, any overprint must be acquired within a single geomagnetic polarity epoch. The Milton overprint was acquired during a particularly long epoch, the Cretaceous normal superchron (119–84 Ma). The maximum allowable  $t_r$  is about half the length of the superchron or 20 Ma, giving a lower limit of 135°C for the maximum paleotemperature  $T_r$  during remagnetization (Fig. 4).

A minimum value for  $t_r$  is dictated by rates of uplift from depth. The high coal ranks observed in the Sydney Basin imply prolonged burial to 1–3 km depths [1]. Erosional unroofing and isostatic uplift from depth require a time  $t_r$  of at least 10 ka, which from Fig. 4 implies an upper limit of 190°C for  $T_r$ .

The range of possible paleotemperatures could be narrowed further if the constraints were tighter. For example, overprinting during a polarity chron of typical length would reduce the maximum  $t_r$  value to  $\approx 1$  Ma. For the same ( $t_L$ ,  $T_L$ ) values used in Fig. 4, this would raise the lower limit on  $T_r$  to 140°C. Likewise, one could argue that maximum  $T_r$  is experienced during prolonged residence at maximum depth, which for coalification requires  $t_r$  to be much longer than 10 ka. This would lower the upper limit on  $T_r$ .

#### 4. Combining remagnetization data for pyrrhotite and magnetite

In order to determine the most probable combination of  $T_r$  and  $t_r$  without imposing any external constraints, we next combine remagnetization data for both pyrrhotite and magnetite. We use only  $T_L$  values for single-domain grains because

Néel's theory [16] applies only to such grains. This requirement is easier to satisfy for pyrrhotite, whose critical grain size  $d_0$  for single-domain behavior is 1–2  $\mu\text{m}$  [26], than for magnetite, with  $d_0 = 0.05\text{--}0.1 \mu\text{m}$  [21].

In the Milton Monzonite, there are four main groupings of  $T_L$  values ([23] fig. 2): 200–230°C; 280–330°C; 400–440°C; and 510–550°C. Group 1 samples contain pyrrhotite, as described earlier. Group 2 samples contain single-domain magnetite (an example is sample 2e4 in Fig. 3). Group 3 and 4 samples contain multidomain grains or mixed single-domain and multidomain grains of magnetite [23].

$T_L$  values for multidomain grains are anomalously high [23] compared to the predictions of Eq. 2. However,  $T_L$  values for groups 3 and 4 are reduced to the same range as group 2 by prior low temperature demagnetization (LTD), consisting of zero-field cooling through the magnetite isotropic point at 130 K. For example, sample 2f2, treated with prior LTD, has  $T_L = 291^\circ\text{C}$  (Fig. 3), whereas its companion specimens 2f1 and 2f5 which were not treated with LTD have  $T_L$  values above 350°C. LTD has the effect of unpinning domain walls, thereby demagnetizing multidomain NRM, while leaving single-domain NRM pinned by shape anisotropy largely intact [27–30]. For paleotemperature determination, we used only  $T_L$  values from groups 1 and 2, plus data for LTD-treated samples.

In Fig. 4, the minimum, average, and maximum  $T_L$  values for pyrrhotite- and magnetite-bearing samples, (200, 215, 230°C) and (280, 305, 330°C), respectively, are anchored by the horizontal line  $t_L \approx 5$  min. The most probable combination ( $T_r$ ,  $t_r$ ) is the intersection point of the average pyrrhotite and magnetite contours:  $T_r \approx 165^\circ\text{C}$  and  $t_r \approx 100$  ka. Incorporating our previous upper and lower bounds for  $T_r$ , we estimate that the Milton region was heated to a peak temperature of  $165 \pm 30^\circ\text{C}$  during remagnetization.

If a value of 10 min was used instead for  $t_L$ , the upper and lower bounds on  $T_r$  would increase by  $\approx 2^\circ\text{C}$  (determined by the shift in pyrrhotite contours) but the most probable  $T_r$  would actually decrease by  $\approx 3^\circ\text{C}$  (because the intersecting magnetite contour shifts upward more than the aver-

age pyrrhotite contour). Thus the  $T_r$  estimates are insensitive to small uncertainties in  $t_L$ .

We avoided long hold times in order to minimize chemical alteration. However, had we used larger values of  $t_L$ , lower  $T_L$  values would have been measured. These ( $t_L$ ,  $T_L$ ) data, in combination with the shifted contours, would lead to  $T_r$  estimates similar to those reported here. In other words, the method can be expected to work equally well for long or short hold times.

Notice that the upper and lower bounds on  $T_r$  are determined by the pyrrhotite contours alone. The magnetite contours are more oblique and would set broader limits on  $T_r$ . For this reason, pyrrhotite data and the newly calculated pyrrhotite  $T$ - $t$  contours are particularly valuable in setting bounds on ranges of plausible paleotemperatures.

## 5. Comparison with earlier studies

In an earlier remagnetization study, Middleton and Schmidt [1] compared magnetite  $T_L$  data for the Milton Monzonite with hematite  $T_L$  data for the Patonga Claystone (near the coast south of Newcastle in Fig. 2). Both units fall between the 0.7% and 0.8% vitrinite reflectance contours, but they are geographically widely separated. The estimated  $T_r$  was 250–300°C for a duration of heating  $t_r$  of several million years [1]. Shorter durations of heating would drive the paleotemperature estimate still higher. The contours used a different remagnetization theory [31]; however, using the Néel [7,16] contours gave even higher  $T_r$  estimates. One problem could be combining data from widely separated parts of the Sydney Basin but the most probable reason is the use of uncorrected magnetite  $T_L$  values, most of which are anomalously high because of the presence of multidomain grains [23].

Middleton and Schmidt [1] independently estimated maximum paleotemperatures of surface rocks in the Sydney Basin using vitrinite reflectance data. Assuming residence times for coalification of 70–110 Ma, their estimates were  $\approx 100\text{--}200^\circ\text{C}$  using a paleogeothermal gradient of 70°C/km typical of heat flow in incipient or young rifts,

such as the Rio Grande Rift and the Red Sea [32,33]. Middleton and Schmidt recognized that these temperatures were significantly less than those estimated from the magnetic overprinting, but argued that ‘coalification depends on long duration of heating, whereas overprint magnetizations reflect elevated temperatures’, possibly of briefer duration.

Our work negates this view. The  $T_r$  estimate of  $165 \pm 30^\circ\text{C}$ , using the Néel–Pullaiah [7,16] remagnetization contours for pyrrhotite and magnetite, is very comparable to values from vitrinite studies. Coalification and magnetic overprinting seem to respond in similar ways to long-term burial, although the relationship between vitrinite reflectance, time and temperature (Eq. 3 of [1]) is more complicated than the first-order Arrhenius law describing thermoviscous remagnetization (Eq. 1 of this paper). The earlier magnetic overestimates of  $T_r$  likely were biased by multidomain grains. Our approach thus reconciles previously divergent estimates of paleotemperatures during deep burial based on coal maturity and on remagnetization.

## 6. Advantages and limitations of the remagnetization geothermometer

Our methodology is new in two respects. First, it uses remagnetization data from a single formation, eliminating uncertainties about possible differences in paleotemperatures in different parts of a sedimentary basin. Second, it makes use of  $T_L$  data and remagnetization contours for pyrrhotite which are much less sensitive to the choice of remagnetization time  $t_r$  than are the corresponding data and contours for magnetite.

In fact, the pyrrhotite contours used by themselves set the lower and upper bounds on  $T_r$  (see Fig. 4). Pyrrhotite is of special importance because remagnetization temperatures in the 100–300°C (i.e. 373–573 K) range are close to the pyrrhotite Curie point of 320°C (593 K), so that  $M_s$  and  $\beta$  change rapidly with  $T$ , producing steep  $T$ – $\tau$  contours. Magnetite in the same temperature range is far from its Curie point, so that  $M_s$  and  $\beta$  change slowly with  $T$ , producing gently sloping  $T$ – $\tau$  contours.

The remagnetization method of estimating paleotemperature has some advantages over conventional estimates based on organic or clay diagenesis, color changes in microfossils, and petrographic observations of hydrothermal or metamorphic minerals. It requires only basic paleomagnetic instrumentation. Any igneous, sedimentary or metamorphic rock with a pre-existing NRM (not necessarily primary) and a thermal overprint can be used. Pyrrhotite is the preferred NRM carrier because its  $T$ – $t$  contours are steep, but magnetite is usable if  $t_r$  can be estimated within one or two orders of magnitude. Finally, the vector direction of the overprint yields a paleomagnetic pole that dates the time of remagnetization.

There are two principal difficulties in using the remagnetization method. The first is locating suitably overprinted formations, particularly ones in which the thermoviscous overprint is carried by pyrrhotite. Although these are generally considered to be rare, there are a number of examples [18,34,35] from mountain belts, and pyrrhotite is increasingly being recognized as an important magnetic mineral in other settings as well. Secondly, one must ensure that the thermal overprint is carried by single-domain grains. This requirement is not too difficult to satisfy for pyrrhotite, high Ti titanomagnetite, or hematite, all of which have critical single-domain sizes  $d_0 > 1 \mu\text{m}$ , but it is a problem with magnetite, for which  $d_0$  is 0.05–0.1  $\mu\text{m}$ . Reliable  $T$ – $t$  contours cannot be found for multidomain magnetite because a particular  $T_B$  has a spectrum of unblocking temperatures rather than a single  $T_{UB}$  as in single-domain grains [36,37]. However, LTD prior to thermal demagnetization is effective in reducing  $T_L$  to single-domain levels and is quick to perform using liquid  $\text{N}_2$  on batches of samples.

## 7. Paleogeothermal gradient and depth of burial estimates

In analyzing sedimentary basins or metamorphic terrains, one would like to know not only paleotemperature but also paleogeothermal gradient and depth of burial. Neither is given directly

by paleomagnetic methods. However, if an independent mineral geobarometer can be found [4], one can calculate the paleogeothermal gradient, which may have important implications for the tectonic mechanism of burial/uplift (e.g. pre-rifting thermal uplift of a plate margin, subduction followed by arc migration, Tibetan-style collision and crustal thickening). Conversely, if a reasonable value can be inferred for paleogeothermal gradient,  $T_r$  yields maximum burial depth.

Burial depths of presently exposed Sydney Basin rocks estimated from vitrinite reflectance data range from 0.9 to 2.9 km [1]. Our estimate of burial depth for the Milton region, combining the paleotemperature estimate of  $165 \pm 30^\circ\text{C}$  with a paleogeothermal gradient for young or incipient rifts of  $70^\circ\text{C}/\text{km}$ , is  $2.3 \pm 0.4$  km. The remagnetization estimate is in excellent agreement with the deeper estimates from vitrinite data.

## 8. Conclusions

The thermal remagnetization geothermometer [7,16] has been used mainly with magnetite-bearing rocks and has had two associated problems:

(1) The correction from the demagnetization temperature  $T_L$  of a thermal NRM overprint measured in the laboratory to the corresponding temperature  $T_r$  experienced in nature during remagnetization is usually large, because the  $(T, t)$  contours (Eq. 1 and Fig. 1) are gently sloping when  $T_r$  is far below the magnetite Curie point of  $580^\circ\text{C}$ .

(2)  $T_L$  values measured for multidomain magnetite, the typical grain size range in many rocks, are anomalously high compared to single-domain  $T_L$  values assumed in remagnetization theory. This in turn makes the paleotemperature  $T_r$  estimates anomalously high. There is unfortunately no simple means of ‘correcting’ multidomain  $T_L$  values [36,37].

The pyrrhotite remagnetization geothermometer presented in this paper (Figs. 1, 4) improves matters considerably. The typical range of remagnetization temperatures is close to the pyrrhotite Curie temperature of  $320^\circ\text{C}$ , leading to steep  $(T, t)$  contours and a smaller correction from  $T_L$  to

$T_r$ . Furthermore, single-domain pyrrhotite is much commoner in nature than single-domain magnetite because the pyrrhotite single-domain threshold size is around  $1\text{--}2 \mu\text{m}$ , an order of magnitude larger than for magnetite. Therefore the problem of anomalous multidomain values of  $T_L$  is much less severe than for magnetite.

We also propose a method of circumventing the problem of anomalously high  $T_L$  values in magnetite-bearing samples. Rather than attempting to correct these values by some theoretical relation (a fruitless task, since a single  $T_B$  for a multidomain grain has a spectrum of  $T_{UB}$  values [36,37]), we have found it effective to pre-treat samples by zero-field cycling to liquid  $\text{N}_2$  temperature (low temperature demagnetization or LTD). LTD greatly reduces the NRM of multidomain grains in a mixture of grain sizes, and usually reduces originally high  $T_L$  values to single-domain levels [23]. The thermal remagnetization geothermometer is then usable.

Pyrrhotite is not as common a remanence carrier as magnetite, but where it occurs [18,34,35], it is the mineral of choice for remagnetization geothermometry. The pyrrhotite  $(T, t)$  contours in Figs. 1 and 4 are much steeper than magnetite (or hematite) contours, and set much narrower limits on burial temperature when minimum and maximum times for remagnetization are constrained by factors like uplift time, coalification, and lengths of polarity chrons. In the ideal situation where two minerals carry the same thermal NRM overprint, a unique  $(T_r, t_r)$  can be estimated without other input, but generally geological and geomagnetic constraints are needed to set upper and lower bounds on remagnetization temperature. Because time enters Eq. 1 as a logarithmic factor, the constraints on time do not need to be particularly tight.

The test case presented in this paper demonstrates the usefulness of the technique. The Milton Monzonite and its surroundings are estimated (using mainly overprint data for pyrrhotite) to have been reheated and remagnetized (around 100 Ma BP) at  $T_r = 165 \pm 30^\circ\text{C}$ , in excellent agreement with estimates from vitrinite reflectance data [1]. Former much higher magnetic estimates of  $T_r$  [1] were flawed by anomalously high multidomain  $T_L$



values. Using a reasonable estimate for paleogeothermal gradient, the depth of burial is calculated to have been  $2.3 \pm 0.4$  km, again in excellent agreement with vitrinite estimates for this part of the Sydney Basin.

### Acknowledgements

We thank Randy Enkin and Mike Jackson for helpful reviews that led to improvements in the paper. Two of us (D.J.D. and Ö.Ö.) are grateful to CSIRO for support during their stay as visiting scientists. Most of the data analysis and calculations were done at Toronto with support from Natural Sciences and Engineering Research Council of Canada grant A7709. [RV]

### References

- [1] M.F. Middleton, P.W. Schmidt, Paleothermometry of the Sydney Basin, *J. Geophys. Res.* 87 (1982) 5351–5359.
- [2] J. Hower, E.V. Eslinger, M.E. Hower, E.A. Perry, Mechanism of burial and metamorphism of argillaceous sediment: 1. Mineralogical and chemical evidence, *Geol. Soc. Am. Bull.* 87 (1976) 725–737.
- [3] F.D. Legall, C.R. Barnes, R.W. Macqueen, Thermal maturation, burial history and hotspot development, Paleozoic strata of southern Ontario-Quebec, from conodont and acritarch colour alteration studies, *Bull. Can. Petrol. Geol.* 29 (1981) 492–539.
- [4] L.M. Anovitz, E.J. Essene, Thermobarometry and pressure-temperature paths in the Grenville Province of Ontario, *J. Petrol.* 31 (1990) 197–241.
- [5] D. York, Cooling histories from  $^{40}\text{Ar}/^{39}\text{Ar}$  age spectra: Implications for Precambrian plate tectonics, *Annu. Rev. Earth Planet. Sci.* 12 (1984) 383–409.
- [6] M.E. Moore, A.J.W. Gleadow, J.F. Lovering, Thermal evolution of rifted continental margins: New evidence from fission tracks in basement apatites from southeastern Australia, *Earth Planet. Sci. Lett.* 78 (1986) 255–270.
- [7] G. Pullaiah, E. Irving, K.L. Buchan, D.J. Dunlop, Magnetization changes caused by burial and uplift, *Earth Planet. Sci. Lett.* 28 (1975) 133–143.
- [8] M.H. Dodson, E. McClelland-Brown, Magnetic blocking temperature of single domain grains during slow cooling, *J. Geophys. Res.* 85 (1980) 2625–2637.
- [9] E.J. Schwarz, Depth of burial from remanent magnetization: The Sudbury irruptive at the time of diabase intrusion (1250 Ma), *Can. J. Earth Sci.* 14 (1977) 82–88.
- [10] R. Van der Voo, S.G. Henry, H.N. Pollack, On the significance and utilization of secondary magnetizations in red beds, *Phys. Earth Planet. Int.* 16 (1978) 12–19.
- [11] P.W. Schmidt, B.J.J. Embleton, Magnetic overprinting in southeastern Australia and the thermal history of its rifted margin, *J. Geophys. Res.* 86 (1981) 3998–4008.
- [12] D.V. Kent, Thermoviscous remagnetization in some Appalachian limestones, *Geophys. Res. Lett.* 12 (1985) 805–808.
- [13] M. Jackson, R. Van der Voo, Thermally activated viscous remanence in some magnetite- and hematite-bearing dolomites, *Geophys. Res. Lett.* 13 (1986) 1434–1437.
- [14] D.V. Kent, J.D. Miller, Red beds and thermoviscous remagnetization theory for hematite, *Geophys. Res. Lett.* 14 (1987) 327–330.
- [15] K.L. Buchan, E.J. Schwarz, Determination of the maximum temperature profile across dyke contacts using remanent magnetization and its applications, in: H.C. Halls, W.F. Fahrig (Eds.), *Mafic Dyke Swarms*, Geol. Assoc. Can. Spec. Pap. 34 (1987) 221–227.
- [16] L. Néel, Théorie du traînage magnétique des ferromagnétiques en grains fins avec applications aux terres cuites, *Ann. Géophys.* 5 (1949) 99–136.
- [17] D.A. Clark, Magnetic properties of pyrrhotite, M.Sc. thesis, University of Sydney, 1983, 256 pp.
- [18] C. Crouzet, G. Ménard, P. Rochette, High-precision three-dimensional paleothermometry derived from paleomagnetic data in an Alpine metamorphic unit, *Geology* 27 (1999) 503–506.
- [19] A. Menyeh, W. O'Reilly, The coercive force of fine particles of monoclinic pyrrhotite ( $\text{Fe}_7\text{S}_8$ ) studied at elevated temperatures, *Phys. Earth Planet. Int.* 89 (1995) 51–62.
- [20] A. Menyeh, W. O'Reilly, Thermoremanent magnetization in monodomain monoclinic pyrrhotite  $\text{Fe}_7\text{S}_8$ , *J. Geophys. Res.* 101 (1996) 25045–25051.
- [21] D.J. Dunlop, Ö. Özdemir, *Rock Magnetism: Fundamentals and Frontiers*, Cambridge University Press, New York, 1997, 573 pp.
- [22] D.J. Dunlop, P.W. Schmidt, Ö. Özdemir, D.A. Clark, Paleomagnetism and paleothermometry of the Sydney Basin: 1. Thermoviscous and chemical overprinting of the Milton Monzonite, *J. Geophys. Res.* 102 (1997) 27271–27283.
- [23] D.J. Dunlop, Ö. Özdemir, P.W. Schmidt, Paleomagnetism and paleothermometry of the Sydney Basin: 2. Origin of anomalously high unblocking temperatures, *J. Geophys. Res.* 102 (1997) 27285–27295.
- [24] D.J. Dunlop, On the use of Zijderveld vector diagrams in multicomponent paleomagnetic studies, *Phys. Earth Planet. Int.* 20 (1979) 12–24.
- [25] E.J. Schwarz, K.L. Buchan, Identifying types of remanent magnetization in igneous contact zones, *Phys. Earth Planet. Int.* 58 (1989) 155–162.
- [26] A. Menyeh, W. O'Reilly, The magnetization process in monoclinic pyrrhotite ( $\text{Fe}_7\text{S}_8$ ) particles containing few domains, *Geophys. J. Int.* 104 (1991) 387–399.
- [27] R.T. Merrill, Low-temperature treatment of magnetite

- and magnetite-bearing rocks, *J. Geophys. Res.* 75 (1970) 3343–3349.
- [28] F. Heider, D.J. Dunlop, H.C. Soffel, Low-temperature and alternating field demagnetization of saturation remanence and thermoremanence in magnetite grains (0.037  $\mu\text{m}$  to 5 mm), *J. Geophys. Res.* 97 (1992) 9371–9381.
- [29] S.L. Haldedahl, R.D. Jarrard, Low temperature behavior of single-domain through multidomain magnetite, *Earth Planet. Sci. Lett.* 130 (1995) 127–139.
- [30] Ö. Özdemir, D.J. Dunlop, Single-domain-like behavior in a 3-mm natural single crystal of magnetite, *J. Geophys. Res.* 103 (1998) 2549–2562.
- [31] D. Walton, Time-temperature relations in the magnetization of assemblies of single domain grains, *Nature* 286 (1980) 245–247.
- [32] A.J. Erickson, R.P. Von Herzen, J.G. Girdler, B.V. Marshall, R. Hyndman, Geothermal measurements in deep-sea drill cores, *J. Geophys. Res.* 80 (1975) 2515–2528.
- [33] E.R. Decker, S.B. Smithson, Heat flow and gravity interpretation across the Rio Grande rift in southern New Mexico and west Texas, *J. Geophys. Res.* 80 (1975) 2542–2552.
- [34] P. Rochette, G. Ménard, R. Dunn, Thermochronometry and cooling rates deduced from single sample records of successive magnetic polarities during uplift of metamorphic rocks in the Alps (France), *Geophys. J. Int.* 108 (1992) 491–501.
- [35] C. Crouzet, P. Rochette, G. Ménard, M. Prévot, Acquisition d'aimantations thermorémanentes partielles successives par la pyrrhotite monodomaine lors du refroidissement de la zone dauphinoise interne, *C.R. Acad. Sci. Paris* 325 (1997) 643–649.
- [36] D.J. Dunlop, S. Xu, Theory of partial thermoremanent magnetization in multidomain grains, 1. Repeated identical barriers to wall motion (single microcoercivity), *J. Geophys. Res.* 99 (1994) 9005–9023.
- [37] S. Xu, D.J. Dunlop, Theory of partial thermoremanent magnetization in multidomain grains, 2. Effect of microcoercivity distribution and comparison with experiment, *J. Geophys. Res.* 99 (1994) 9025–9033.